Relativistic quantum chemistry on quantum computers

Libor Veis,[1, 2, *] Jakub Višňák,[1] Timo Fleig,[3] Stefan Knecht,[4] Trond Saue,[3] Lucas Visscher,[5] and Jiří Pittner[1, †]

[1] *J. Heyrovský Institute of Physical Chemistry, ASCR, 18223 Prague, Czech Republic*
[2] *Department of Physical and Macromolecular Chemistry, Charles University, 12840 Prague, Czech Republic*
[3] *Laboratoire de Chimie et Physique Quantiques, Université Toulouse 3, IRSAMC, F-31062 Toulouse, France*
[4] *Department of Physics and Chemistry, University of Southern Denmark, DK-5230 Odense M, Denmark*
[5] *Amsterdam Center for Multiscale Modeling, VU University Amsterdam, NL-1081 HV Amsterdam, Netherlands*
(Dated: November 16, 2011)

Last years witnessed a remarkable interest in application of quantum computing for solving problems in quantum chemistry more efficiently than classical computers allow. Very recently, even first proof-of-principle experimental realizations have been reported. However, so far only the non-relativistic regime (i.e. Schroedinger equation) has been explored, while it is well known that relativistic effects can be very important in chemistry. In this letter we present the first quantum algorithm for relativistic computations of molecular energies. We show how to efficiently solve the eigenproblem of the Dirac-Coulomb Hamiltonian on a quantum computer and demonstrate the functionality of the proposed procedure by numerical simulations of computations of the spin-orbit splitting in the SbH molecule. Finally, we propose quantum circuits with 3 qubits and 9 or 10 CNOTs, which implement a proof-of-principle relativistic quantum chemical calculation for this molecule and might be suitable for an experimental realization.

Quantum computing [1] is undoubtedly one of the fastest growing fields of computer science nowadays. Recent huge interest in this interdisciplinary field has been fostered by the prospects of solving certain types of problems more effectively than in the classical setting [2, 3]. The prominent example is the integer factorization problem where quantum computing offers an exponential speedup over its classical counterpart [2]. But it is not only cryptography that can benefit from quantum computers. As was first proposed by R. Feynman [4], quantum computers could in principle be used for *efficient* simulation of another quantum system. This idea, which employs mapping of the Hilbert space of a studied system onto the Hilbert space of a register of quantum bits (qubits), both of them being exponentially large, can in fact be adopted also in quantum chemistry.

Several papers using this idea and dealing with the interconnection of quantum chemistry and quantum computing have appeared in recent years. These cover: calculations of thermal rate constants of chemical reactions [5], *non-relativistic* energy calculations [6–9], quantum chemical dynamics [10], calculations of molecular properties [11], initial state preparation [12, 13], and also first proof-of-principle experimental realizations [14, 15]. An interested reader can find a comprehensive review in [16].

An *efficient* (polynomially scaling) algorithm for calculations of *non-relativistic* molecular energies, that employs the phase estimation algorithm (PEA) of Abrams and Lloyd [17], was proposed in the pioneering work by Aspuru-Guzik, et al. [6]. When the ideas of measurement based quantum computing are adopted [18], the phase estimation algorithm can be formulated in an iterative manner [iterative phase estimation (IPEA)] with only one read-out qubit [8, 9]. If the phase ϕ ($0 \leq \phi < 1$), which is directly related to the desired energy [9], is expressed in

the binary form: $\phi = 0.\phi_1\phi_2\ldots$, $\phi_i = \{0, 1\}$, one bit of ϕ is measured on the read-out qubit at each iteration step. The algorithm is iterated backwards from the least significant bits of ϕ to the most significant ones, where the k-th iteration is shown in Figure 1. Not to confuse the reader, $\hat{H}$ in the exponential denotes the Hamiltonian operator, whereas H (in a box) denotes the standard single-qubit Hadamard gate. $|\psi_{\text{system}}\rangle$ represents the part of a quantum register that encodes the wave function of a studied system, R_z is a z-rotation gate whose angle ω_k depends on the results of the previously measured bits [8, 9], and parameter τ ensures that $0 \leq \phi < 1$. The PEA always needs an initial guess of the wave function corresponding to the desired energy. This can be either the result of some approximate, polynomially scaling *ab initio* method [7, 9], or as originally proposed by Aspuru-Guzik, et al. [6] the exact state or its approximation prepared by the adiabatic state preparation (ASP) method.
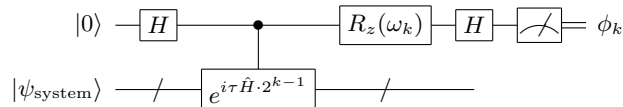

Figure 1. The k-th iteration of the iterative phase estimation algorithm (IPEA). The feedback angle ω_k depends on the previously measured bits.

It is a well known fact that an accurate description of molecules with heavy elements requires adequate treatment of relativistic effects [19]. The most rigorous approach [besides the quantum electrodynamics (QED) which is not feasible for quantum chemical purposes] is the four component (4c) formalism [20]. However, this concept brings three major computational difficulties: (1) working with 4c orbitals (bispinors), (2) complex algebra when molecular symmetry is low, and (3) rather large Hamiltonian matrix eigenvalue problems [due to

larger mixing of states than in the non-relativistic (NR) case]. The central objective of this work is thus to address these problems in regard of an application of a quantum computer and the extension of the quantum full configuration interaction (qFCI) method to the relativistic regime. We would like to note here that in all simulations presented henceforth, we restricted ourselves to the 4c Dirac-Coulomb Hamiltonian:

$$\hat{H} = \sum_{i=1}^{N} \left[c(\boldsymbol{\alpha}_i \cdot \mathbf{p}_i) + \beta_i' m c^2 + \sum_A \frac{1}{r_{iA}} \right] + \sum_{i<j} \frac{1}{r_{ij}}$$

$$\alpha_k = \begin{pmatrix} 0 & \sigma_k \\ \sigma_k & 0 \end{pmatrix}, \quad \beta' = \beta - I_4, \quad \beta = \begin{pmatrix} I_2 & 0 \\ 0 & -I_2 \end{pmatrix},$$

where σ_k ($k = x, y, z$) are Pauli matrices and I_2 the 2×2 unit matrix. This type of Hamiltonian covers the major part of the spin-orbit interaction (including two-electron spin-own orbit) and also scalar relativistic effects. It is in fact without loss of generality sufficient for our purposes since going to Dirac-Coulomb-Breit Hamiltonian [20] correct to $\mathcal{O}(c^{-2})$ is conceptually straightforward as the inclusion of the corresponding integrals requires a classically polynomial effort.

We will start the description of the algorithm with a mapping of the relativistic quantum chemical wave function onto a quantum register. The simplest (scalable) NR approach, the direct mapping (DM) [6], assigns each spin orbital one qubit ($|0\rangle$ = unoccupied, $|1\rangle$ = occupied). The relativistic case is very similar due to the no-pair approximation (NPA) [20], which in relativistic quantum chemistry is widely used. In NPA, one builds up an N-electron wave function only from Slater determinants containing positive-energy bispinors. This procedure in fact neglects all QED effects, but it is justifiable at the energy scale relevant to chemistry. Moreover, because of the time-reversal symmetry of the Dirac equation, bispinors occur in degenerate Kramers pairs [20] denoted A and B (analogy to α and β spin in NR treatment) and the relativistic DM thus looks like: one qubit for bispinor A and one for B. The 4c character of molecular bispinors therefore does not complicate the approach substantially [note that as in the NR case, the Hartree-Fock (HF) calculation is done on a classical computer and only the exponentially scaling FCI on a quantum one].

The DM is known to be not optimal as it maps the whole Fock space of the system on the Hilbert space of qubits. For this reason, compact mappings from a subspace of fixed-electron-number and spin- or symmetry-adapted wave functions have been proposed [6, 7]. However, general factorization schemes [i.e. algorithms to systematically generate quantum circuit implementing $\exp(i\tau\hat{H})$] for these mappings have not been discovered yet. In the relativistic case, the most convenient compact mapping is based on a subspace of symmetry-adapted functions employing the double group symmetry.

GAS	Min. el.	Max. el.	Shell types
I	0	4	$\sigma_{1/2}, \pi_{1/2}$
II	2	4	$\pi_{3/2}$
III	4	4	$\sigma_{1/2}^*$, 43 virtual Kramers pairs

Table I. GAS and occupation constraints for SbH $X\ 0^+$ and $A\ 1$ states CI calculations. The minimum and maximum number of electrons are accumulated values - apply to this and all preceding GA spaces.

Assuming the NPA and the empty Dirac picture, the relativistic Hamiltonian has the same second quantized structure as the NR one

$$\hat{H} = \sum_{pq} h_{pq} a_p^\dagger a_q + \frac{1}{2} \sum_{pqrs} g_{pqrs} a_p^\dagger a_q^\dagger a_s a_r,$$

h_{pq} and g_{pqrs} denote one- and two-electron integrals that are now in general complex. This is in fact no difficulty for a quantum computer, since our working environment is a complex vector space of qubits anyway and we do the exponential of a complex matrix even if the Hamiltonian is real (see Figure 1). After the decomposition of the unitary propagator [$\exp(i\tau\hat{H})$] to elementary quantum gates (in case of DM) using the Jordan-Wigner transform [21], one can see that complex molecular integrals require twice as many gates compared to real ones [8], while complex arithmetic on a classical computer requires four times more operations.

The last of the aforementioned difficulties of the 4c formalism is the size of a Hamiltonian matrix eigenvalue problem. When we put the double group symmetry aside and employ Kramers restricted (KR) approach, the relativistic Hamiltonian, unlike the NR one, mixes determinants with different values of the pseudo-quantum number M_K [$M_K = 1/2(N_A - N_B)$, in NR case it is possible to choose M_K as M_S]. It can be shown (see Supporting Information) that the ratio between dimensions of relativistic and non-relativistic Hamiltonian matrices scales as $\mathcal{O}(m^{1/2})$ in the number of molecular orbitals/bispinors.

When employing the DM on a quantum computer, this problem does not occur, since the Hamiltonian (2) then implicitly works with all possible values of M_K. The scaling of the relativistic qFCI method is therefore the same as the NR one, namely $\mathcal{O}(m^5)$ [8, 14], where m is the number of molecular orbitals (bispinors).

For numerical tests of the algorithm, we have chosen the SbH molecule whose non-relativistic ground state $^3\Sigma^-$ splits due to spin-orbit effects into $X\ 0^+$ and $A\ 1$. In the approximate $\lambda\omega$-projection, these states are dominated by $\sigma_{1/2}^2\pi_{1/2}^2\pi_{3/2}^0$ and $\sigma_{1/2}^2\pi_{1/2}^1\pi_{3/2}^1$ configurations. The splitting is truly of "molecular nature" as it disappears for dissociated atoms and its experimental value is $\Delta E_{SO} = 654.97$ cm^{-1} [22].

In all our simulations, we used the Dyall triple-zeta + valence correlating functions, total 28s 21p 15d 1f for Sb and cc-pVTZ (from EMSL basis set library) for H.
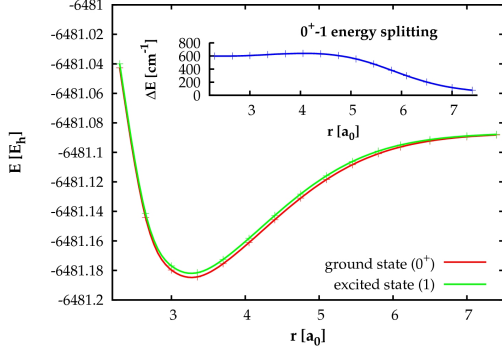
Figure 2. Simulated potential energy curves of ground (0^+) and excited (1) states of SbH, and spin-orbit energy splitting.
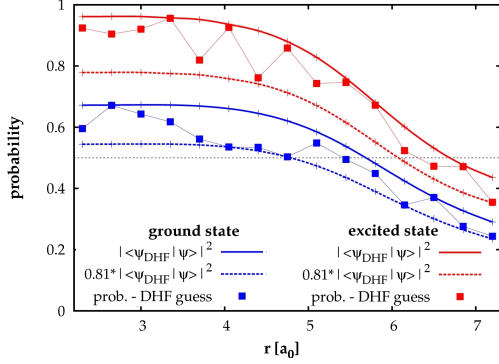

Figure 3. SbH ground (0^+) and excited (1) state qFCI success probabilities (SPs) corresponding to HF initial guesses.

We, of course, could not manage to simulate the FCI calculations with all electrons in such a large basis. We instead simulated general active space (GAS) KRCI computations [23] with the occupation constraints shown in Table I giving rise to CI spaces of approximately 29500 determinants. For a balanced description of both states, we optimized the spinors taking an average energy expression (2 electrons in 2 Kramers pairs $\pi_{1/2}$, $\pi_{3/2}$). We worked solely with a compact mapping employing the double-group symmetry (C_{2v}^*) and exponential of a Hamiltonian was simulated as an n-qubit gate (similarly as in [6, 7, 9]). We used the DIRAC program [24] for calculations of Hamiltonian matrices. Simulations of qFCI computations were performed with our own C++ code [9]. We ran 17 iterations of the IPEA with the difference between max. and min. expected energies equal to $0.5\ E_h$ We also did not count the least significant binary digit of the phase ϕ to the total success probability (for more details of the algorithm, we refer the reader to our preceding paper [9]). This procedure corresponds to the final energy precision $\approx 3.81 \times 10^{-6}\ E_h$.

Simulated potential energy curves of both states are shown in Figure 2. Based on our KRCI setup we obtain a vertical ΔE_{SO} of 617 cm^{-1}. Success probabilities (SPs) of the algorithm with HF initial guesses $(\sigma_{1/2}^2 \pi_{1/2}^2 \pi_{3/2}^0$ for the $X\ 0^+$ state and $\sigma_{1/2}^2 \pi_{1/2}^1 \pi_{3/2}^1$ for $A\ 1$ one) are

presented in Figure 3. They correspond to the IPEA with the second part of a quantum register (encoding the relativistic quantum chemical wave function) maintained during all iterations (in [9] denoted as version **A**). In this case, SPs always lie in the interval $|\langle\psi_{\mathrm{init}}|\psi_{\mathrm{exact}}\rangle|^2 \cdot (0.81, 1\rangle$ [9]. Ground state SPs confirm that relativistic states have, due to near degeneracies caused by the spin-orbit coupling, often a stronger multireference character than non-relativistic ones. The upper bound of the SP is less than 0.7 even for the equilibrium geometry and HF initial guesses can in fact be safely used (SP > 0.5, amplification of SP by repetitions) only up to 4.8 a_0. The SPs of the $A\ 1$ state are higher and HF initial guesses can be in a noise-free environment used up to 6 a_0.

The difficulty connected with a low success probability for the $X\ 0^+$ state at longer distances can be overcome by the ASP method [6]. In this approach, one slowly varies the Hamiltonian of a quantum register, starting with a trivial one with a known eigenstate and ending with the final exact one in a following simple way

$$\hat{H} = (1-s)\hat{H}_{\mathrm{init}} + s\hat{H}_{\mathrm{exact}} \quad s : 0 \to 1. \quad (3)$$

If the change is slow enough (depending on the gap between the ground and the first excited state), the register remains in its ground state according to the adiabatic theorem [25]. In our relativistic example, analogously to the non-relativistic one [6], $\hat{H}_{\mathrm{init}}$ is defined to have all matrix elements equal to zero, except H_{11}, which is equal to the (Dirac-)HF energy.
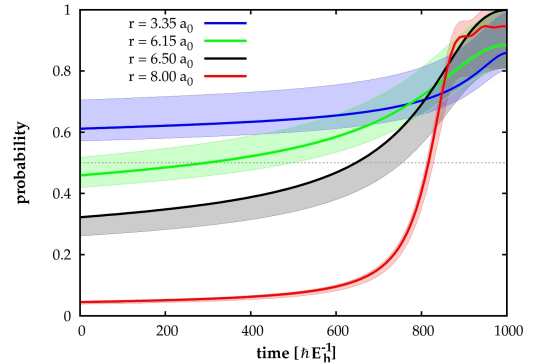

Figure 4. Adiabatic state preparation (ASP) of the SbH ground state (0^+) for different internuclear distances. Solid lines correspond to qFCI success probabilities, $|\langle\psi_{\mathrm{ASP}}|\psi_{\mathrm{exact}}\rangle|^2 \cdot (0.81, 1\rangle$ interval is colored. 1000 $\hbar E_h^{-1} \approx 10^{-14}$ s.

We simulated $X\ 0^+$ qFCI computations with adiabatically prepared states for different internuclear distances, results are shown in Figure 4. In this case, for computational reasons, we employed complete active space (CAS) KRCI method with a CAS composed of 2 electrons in the highest occupied $(\pi_{1/2})$ and 45 lowest unoccupied Kramers pairs (corresponds to 2116 determinants). It can be seen that for $t = 1000\ \hbar E_h^{-1}$, the upper bound of the SP goes safely to unity even for $r = 8\ a_0$.
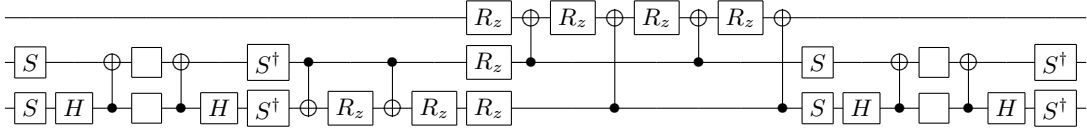
Figure 5. Scheme of a circuit corresponding to CAS(4,3) calculations on SbH. Empty squares represent generic single-qubit gates. R_z gates are without angle specification. For derivation, details, and all the parameters, see Supporting Information.

Recently, there appeared two papers presenting the first physical implementations of *non-relativistic* quantum chemical computations on optical [14] and NMR [15] quantum computers. Correspondingly, we would like to propose two candidates for the first *relativistic* computations on real quantum computers. Both represent calculations of SbH $^3\Sigma^-$ ground state spin-orbit splitting. Since one has to employ rather large basis sets (triple-ζ quality) to get a meaningful result, they again are not true FCI calculations, but FCI calculations in a limited CAS.

The first one corresponds to a CAS composed of 2 electrons in the highest occupied ($\pi_{1/2}$) and the lowest unoccupied ($\pi_{3/2}$) Kramers pairs [CAS(2,2)]. After the factorization of a Hamiltonian according to the Ω quantum number and taking into account only one of the two degenerate z-projections of Ω (for $\Omega = 1$), the size of the CI space is 2 for the ground state (0^+) and 1 for the excited state (1). The excited state is therefore trivial and the calculation of the ground state is in fact a complete analogue of the already mentioned NR computations [14, 15], because it needs just one qubit for the wave function (2 in total). The controlled single-qubit gate can be decomposed using 2 controlled NOTs (CNOTs) [1]. Calculations with this active space yield an $\Delta E_{SO} = 509$ cm^{-1} computed at the experimental equilibrium bond distance of 3.255 a_0.

The second example represents a 3-qubit experiment (2 qubits for the wave function) and employs a CAS composed of 4 electrons in the $\sigma_{1/2}\pi_{1/2}\pi_{3/2}$ Kramers pairs [CAS(4,3)]. It gives a better value of $\Delta E_{SO}(518$ cm$^{-1})$ than CAS(2,3). After Ω factorization, the CI space of the excited state has a dimension 3 and that of the ground state 5. Fortunately, near the equilibrium bond distance, the Hamiltonian matrix of the ground state is to a very good approximation block diagonal (ground state energy difference of the order μE_h), coupling only 3 configurations ($\sigma_{1/2}^2\pi_{1/2}^2\pi_{3/2}^0$, $\sigma_{1/2}^2\pi_{1/2}^0\pi_{3/2}^2$, and $\sigma_{1/2}^0\pi_{1/2}^2\pi_{3/2}^2$). If we take into account only these configurations, both states can be encoded by two qubits.

We used the *Quantum Shannon Decomposition* (QSD) technique [26] and decomposed the controlled action of a two-qubit $\exp(i\tau\hat{H})$. QSD is known to decompose a generic three-qubit gate with the least number of CNOTs (20). A minimal number of CNOTs is very important as their implementations are orders of magnitude more difficult. We found a circuit with 9 CNOTs which is not universal in the sense that the decomposition must be

done for all powers of U individually, or a universal 10-CNOT-circuit. The structure of this circuit is shown in Figure 5. The controlled action of nth power of U is simply done by multiplication of the angles of R_z rotations by n. Details of the decomposition and also all parameters important for a possible experimental realization which correspond to the calculations at internuclear distance 3.255 a_0 can be found in the Supporting Information. The proposed experiments are undoubtedly a challenge for different realizations of quantum computation. We regard experimental verification of the usage of HF initial guesses in a realistic noisy environment and also the performance of both versions of IPEA (**A** and **B**) proposed in [9] as very interesting.

Conclusion. - In this work, we have presented the first quantum algorithm for 4c relativistic FCI energy computations. This algorithm not only achieves an exponential speedup over its classical counterpart, but also has the same cost (in terms of scaling) as its NR analogue. We have proved its functionality by numerical simulations of calculations of the spin-orbit splitting in SbH. We have also proposed and designed the first small-scale experimental realizations of relativistic qFCI computations. Our algorithm can be used stand-alone or as a subroutine of a property algorithm of Kassal et. al. [11] e.g. for calculations of NMR properties.

* libor.veis@jh-inst.cas.cz
† jiri.pittner@jh-inst.cas.cz, corresponding author
[1] M. A. Nielsen and I. L. Chuang, *Quantum Computation and Quantum Information* (Cambridge University Press, 2000).
[2] P. W. Shor, Algorithms for quantum computation: Discrete logarithms and factoring, in *Proceedings of 35th IEEE Symposium on Foundations of Computer Science*, pp. 124–134, , 1994, IEEE Press.
[3] L. K. Groover, Phys. Rev. Lett. **79**, 325 (1997).
[4] R. P. Feynman, Int. J. Theor. Phys. **21**, 467 (1982).
[5] D. A. Lidar and H. Wang, Phys. Rev. E **59**, 2429 (1999).
[6] A. Aspuru-Guzik, A. D. Dutoi, P. J. Love, and M. Head-Gordon, Science **309**, 1704 (2005).
[7] H. Wang, S. Kais, A. Aspuru-Guzik, and M. R. Hoffmann, Phys. Chem. Chem. Phys. **10**, 5388 (2008).

[8] J. D. Whitfield, J. Biamonte, and A. Aspuru-Guzik, Mol. Phys. **109**, 735 (2011).

[9] L. Veis and J. Pittner, J. Chem. Phys. **133**, 194106 (2010).

[10] I. Kassal, S. P. Jordan, P. J. Love, M. Mohseni, and A. Aspuru-Guzik, Proc. Natl. Acad. Sci. **105**, 18681 (2008).

[11] I. Kassal and A. Aspuru-Guzik, J. Chem. Phys. **131**, 224102 (2009).

[12] H. Wang, S. Ashhab, and F. Nori, Phys. Rev. A **79**, 042335 (2009).

[13] N. J. Ward, I. Kassal, and A. Aspuru-Guzik, J. Chem. Phys. **130**, 194105 (2009).

[14] B. P. Lanyon *et al.*, Nature Chemistry **2**, 106 (2010).

[15] J. Du *et al.*, Phys. Rev. Lett. **104**, 030502 (2010).

[16] I. Kassal, J. D. Whitfield, A. Perdomo-Ortiz, M. H. Yung, and A. Aspuru-Guzik, Annu. Rev. Phys. Chem **62**, 185 (2011).

[17] D. S. Abrams and S. Lloyd, Phys.Rev.Lett. **83**, 5162 (1999).

[18] R. B. Griffiths and Chi-Sheng Niu, Phys. Rev. Lett. **76**, 3228 (1996).

[19] B. A. Hess and C. M. Marian, *Computational Molecular Spectroscopy* (Wiley, Sussex, 2000), pp. 169–219.

[20] K. G. Dyall and K. Faegri, *Introduction to Relativistic Quantum Chemistry* (Oxford University Press, New York, 2007).

[21] P. Jordan and E. Wigner, Z. Phys. A **47**, 631 (1928).

[22] K. Balasubramanian, Chem. Rev. **89**, 1801 (1989).

[23] T. Fleig, J. Olsen, and L. Visscher, J. Chem. Phys. **119**, 2963 (2003).

[24] DIRAC, a relativistic ab initio electronic structure program, Release DIRAC08 (2008), written by L. Visscher, H. J. Aa. Jensen, and T. Saue, with new contributions from R. Bast, S. Dubillard, K. G. Dyall, U. Ekström, E. Eliav, T. Fleig, A. S. P. Gomes, T. U. Helgaker, J. Henriksson, M. Iliaš, Ch. R. Jacob, S. Knecht, P. Norman, J. Olsen, M. Pernpointner, K. Ruud, P. Sałek, and J. Sikkema (see http://dirac.chem.sdu.dk).

[25] E. Fahri *et al.*, Science **292**, 472 (2001).

[26] V. V. Shende, S. S. Bullock, and I. L. Markov, IEEE Trans. on Computer-Aided Design **25**, 1000 (2006).

[27] F. Vatan and C. Williams, Phys. Rev. A **69**, 032315 (2004).

[28] V. V. Shende, I. L. Markov, and S. S. Bullock, Phys. Rev. A **69**, 062321 (2004).

[29] A. Daskin and S. Kais, J. Chem. Phys. **134**, 144112 (2011).

SUPPORTING INFORMATION

Size of 4c relativistic FCI eigenvalue problem

In this section, we compare dimensions of non-relativistic and 4c relativistic Hamiltonian matrices. In the NR case, the Hamiltonian matrix is block diagonal according to M_S. Thus for a closed shell system with n electrons in m orbitals, the number of determinants is

$$N_{\text{NR}} = \binom{m}{n/2}\binom{m}{n/2}. \qquad \text{(S1)}$$

The relativistic Hamiltonian mixes determinants with different M_K values and therefore

$$N_{\text{R}} = \binom{2m}{n}. \qquad \text{(S2)}$$

Using Stirling's approximation in the form

$$\ln m! \approx \frac{1}{2}\ln(2\pi m) + m\ln m - m \qquad \text{for } m \to \infty, \text{ (S3)}$$

and setting $m = k \cdot n$, the ratio between the relativistic and non-relativistic number of determinants is given by the expression

$$k_{\text{R/NR}} = \frac{N_{\text{R}}}{N_{\text{NR}}} = \left(\frac{\sqrt{\pi(2k-1)}}{2k}\right) \cdot m^{1/2}. \qquad \text{(S4)}$$

Controlled-U circuit design

In this section, we construct a quantum circuit which corresponds to the controlled action of powers of $U = e^{i\tau\hat{H}}$ (see Figure 1) for a CI space of dimension 3. For this case, we need two qubits to encode the quantum chemical wave function and U has a block diagonal structure with 3×3 block of an exponential of a Hamiltonian and unity on a diagonal to complete the vector space of two qubits.

We use the *Quantum Shannon Decomposition* technique of Shende et. al. [26]. It turns out to be very useful to generalize the concept of controlled gates to quantum multiplexors. A quantum multiplexor is a quantum conditional which acts on target qubit(s) in a different way, according to the state of select qubit(s). If the select qubit is the most significant one, then it has the following matrix form

$$\begin{array}{c}\text{}\end{array} = \begin{pmatrix} U_0 & \\ & U_1 \end{pmatrix}. \qquad \text{(S5)}$$

It performs U_0 on the target qubit if the select qubit is $|0\rangle$ and U_1 if the select qubit is $|1\rangle$. A controlled gate

is a special case where $U_0 = I$. More generally, if U is a quantum multiplexor with s select qubits and t target qubits and the select qubits are most significant, the matrix of U will be block diagonal, with 2^s blocks of size $2^t \times 2^t$.

A controlled 2-qubit U (c-U_{2q}) is a special case of multiplexed U and can be decomposed in the following way [26]

A multiplexed z-rotation in the middle of the circuit on the right-hand side (at this stage without angle specification) is in fact a diagonal matrix with second half of a diagonal equal to a Hermitian conjugate of the first one. The circuit equation (S6) corresponds to the matrix equation

$$\begin{pmatrix} I & \\ & U \end{pmatrix} = \begin{pmatrix} V & \\ & V \end{pmatrix}\begin{pmatrix} D & \\ & D^\dagger \end{pmatrix}\begin{pmatrix} W & \\ & W \end{pmatrix}. \qquad \text{(S7)}$$

Note that right in the equation means left in the circuit as the time in a circuit flows from the left to the right.

We then have

$$I = VDW, \qquad \text{(S8)}$$
$$U = VD^\dagger W, \qquad \text{(S9)}$$
$$U^\dagger = VD^2V^\dagger. \qquad \text{(S10)}$$

A single-multiplexed R_z gate (with angle ϕ_0 for $|0\rangle$ state of a select qubit and ϕ_1 for $|1\rangle$) can be implemented with the following circuit

 , (S11)

since σ_x gates on both sides of R_z turn over the direction of the R_z rotation. If we use this approach for demultiplexing the R_z gate in (S6), we end up (after some simple circuit manipulations) with the following circuit for c-U_{2q}

where

$$\varphi_1 = \frac{1}{4}(\phi_{00} + \phi_{01} + \phi_{10} + \phi_{11}), \qquad \text{(S13)}$$

$$\varphi_2 = \frac{1}{4}(\phi_{00} + \phi_{01} - \phi_{10} - \phi_{11}),$$

$$\varphi_3 = \frac{1}{4}(\phi_{00} - \phi_{01} - \phi_{10} + \phi_{11}),$$

$$\varphi_4 = \frac{1}{4}(\phi_{00} - \phi_{01} + \phi_{10} - \phi_{11}).$$

Individual ϕ's in (S13) can be extracted from the diagonal of D, which has the form: $\mathrm{diag}(e^{-i\phi_{00}}, e^{-i\phi_{01}}, e^{-i\phi_{10}}, e^{-i\phi_{11}})$.

We would like to emphasize that this is not intended to be a decomposition technique for general U's, as it itself requires classical diagonalization [of $U^\dagger$, see (S10)]. A general *efficient* decomposition of an exponential of a Hamiltonian to elementary gates is known only for the direct mapping [8, 14]. But this mapping is not suitable for small scale experiments due to the relatively high number of required qubits and operations thereon. Our aim was in fact to prepare the ground for a first *non-trivial* (more than one qubit in the quantum chemical part of the register) experimental realization of (relativistic) quantum chemical computation on a quantum computer.

Because V belongs to the group $\mathbf{O}(4)$ (matrix of eigenvectors of a symmetric matrix), it can be decomposed using only two CNOT gates [27]:

 (S14)
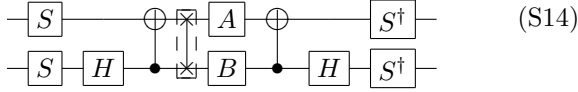
H and S are standard Hadamard and phase gates and A, B are generic single-qubit gates that can be further decomposed e.g. by Z-Y decomposition [1]

$$A = e^{i\alpha} R_z(\beta) R_y(\gamma) R_z(\delta). \qquad \text{(S15)}$$

There is a highlighted swap gate in (S14) which should be applied only if the determinant of V is equal to -1 [27].

The matrix W, on the other hand, is not real as it is equal to $D^\dagger V^\dagger$ (S8) and can be implemented using three CNOT gates (see e.g. [27, 28]). The total count is thus 9 CNOTs.

The disadvantage of the aforementioned scheme is that W must be decomposed for each power of U individually. If we separate W to $V^\dagger$ and $D^\dagger$, $V^\dagger$ is the same for all powers of U (eigenvectors don't change) and $D^\dagger$ can be up to a non-measurable global phase implemented with the following circuit

 (S16)
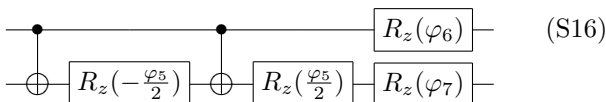
	Ground state (0^+)	Excited state (1)
ϕ_{00}	-1.01642278	-1.00656763
ϕ_{01}	-0.68574813	-0.18597924
ϕ_{10}	0.69657237	-0.39129153
ϕ_{11}	0	0
β	0.73125768	-0.00680941
γ	-0.10311594	2.21832498
δ	-0.12107336	-3.13494247
$\Delta E_{\mathrm{shift}}$	-6477.89247780	-6477.89247780

Table SI. Circuit parameters: rotation angles ϕ_{ij}, $i, j \in \{0, 1\}$ (S13,S17), Z-Y decomposition parameters of A, B (S14) and energy shifts (core energy + nuclear repulsion) for CAS(4,3) calculations of 0^+ and 1 states. For the details see preceding text.

where

$$\varphi_5 = \frac{1}{2}(\phi_{00} - \phi_{01} - \phi_{10} + \phi_{11}),$$

$$\varphi_6 = \frac{1}{4}(-\phi_{00} - \phi_{01} + \phi_{10} + \phi_{11}), \qquad \text{(S17)}$$

$$\varphi_7 = \frac{1}{2}(-\phi_{00} + \phi_{01}).$$

The circuit for $V^\dagger$ is the same as for V (S14), merely A is replaced by $B^\dagger$ and B by $A^\dagger$.

Presented 10-CNOT-circuit is universal for all powers of U. The only thing one has to do is to multiply the angles of R_z rotations in (S12) and (S16) according to the power of U, e.g. by 2 for the second power.

Table SI summarizes the circuit parameters for ground as well as excited state calculations described in the preceding text. Notice that ϕ_{11} is zero in both cases by construction. To complete the vector space of two qubits, we in fact added one eigenvalue of the Hamiltonian equal to zero. Other simplification, which originates from the block diagonal structure of U, is that A and B matrices in the decomposition of V (S14) differ only in a global phase. Because the global phase is not measurable, we present just the angles of rotations. Also only the parameters corresponding to A and B are shown. Going to their Hermitian conjugates means swapping of β and δ and changing the sign of all of them.

For the excited state, the determinant of V is equal to -1 and therefore the swap gate in (S14) should be applied. Because we took Hamiltonian matrices from the DIRAC program [24], the parameters in Table SI refer to the difference between the total energy and core energy + nuclear repulsion ($\Delta E_{\mathrm{shift}}$). The difference between maximum and minimum expected energies [9], which affects the exponential factor τ, was in both cases 1.5 E_h.

We don't give any explicit proof that the *Quantum Shannon decomposition* is optimal in the number of CNOT gates for the specific case of block diagonal c-U_{2q}. However, this conjecture is supported by the fact that we

also implemented the Group Leaders Optimization Algorithm (GLOA) of Dashkin and Kais [29] and unsuccessfully tried to find a better circuit (in terms of number of controlled operations) with a fidelity error smaller than 0.01.